Fatigue of Kidney Stones with Heterogeneous Microstructure Subjected to Shock-Wave Lithotripsy

T. I. Zohdi, A. J. Szeri

Department of Mechanical Engineering, University of California, Berkeley, California 94720

Received 9 November 2004; revised 21 January 2005; accepted 25 January 2005
Published online 8 August 2005 in Wiley InterScience (www.interscience.wiley.com). DOI: 10.1002/jbm.b.30307

Abstract: In this article a theoretical framework is developed for the mechanics of kidney stones with an isotropic, random microstructure—such as those comprised of cystine or struvite. The approach is based on a micromechanical description of kidney stones comprised of crystals in a binding matrix. Stress concentration functions are developed to determine load sharing of the particle phase and the binding matrix phase. Measurements have shown the inclusions to be considerably harder than the binder; consequently, loading of a stone leads to higher stresses in the inclusions than in the binder. As an illustration of the theory, the fatigue of kidney stones subject to shock-wave lithotripsy is considered. Stress concentration functions are used to construct fatigue-life estimates for each phase, as a function of the volume fraction and of the mechanical properties of the constituents, as well as the loading from SWL. The failure of the binding matrix, or of the particulate phase, is determined explicitly in a model for the accumulation of distributed damage. The theory can be used to assess the importance of microscale heterogeneity on the comminution of renal calculi, and to estimate the number of cycles to failure in terms of measurable material properties. © 2005 Wiley Periodicals, Inc. J Biomed Mater Res Part B: Appl Biomater 75B: 351–358, 2005

Keywords: fatigue; microdamage; stress

INTRODUCTION

Shock-wave lithotripsy (SWL) has become the primary technique to treat kidney stones. A large percentage of kidney stones are treated by SWL alone and SWL combined with other treatments. Thousands of shocks are required to break stones to small enough sizes for natural elimination from the body.

There remains much scientific investigation on the precise mechanisms of stone comminution. However, central to the process appears to be the passage of stress waves through the stone, and the erosion of stone surface by cavitation damage from imploding microbubbles.[1,2] It may be that a number of mechanisms interact to produce breakup, working in concert with one another. Whatever the origin of the stresses, the process of stone comminution has been described as one of brittle fracture, for example in Lokhandwalla and Sturtevant[3] and in Coleman and Saunders.[4] As such, the process has been analyzed with the use of a one-dimensional cohesive zone model for a homogeneous material that can fragment into two pieces.[3] Lokhandwalla and Sturtevant were able to estimate the number of shock waves to failure.

The present work is similar in spirit to that of Lokhandwalla and Sturtevant, with a number of further enhancements. Here a theoretical framework capable of treating the heterogeneous microstructure of real kidney stones is presented. A three-dimensional material that is heterogeneous on the microscale is considered. The approach is based on a micromechanical description of those types of kidney stones (reviewed below) comprised of agglomerated isotropic particles, with a binding matrix (Figure 1). The presence of a binder phase and inclusions leads to stress concentrations (or differential load sharing) in a mean sense that can be estimated. After the stress concentrations for material properties derived from experiments are developed, fatigue damage of an initially flawless sample of material is considered. The goal is to analyze the development of damage in an *overall* sense. Stress concentration functions are used to construct fatigue-life estimates for each phase, as a function of the volume fraction and of the mechanical properties of the constituents, as well as the mean and fluctuating loading. The failure of the binding matrix, which is the key requirement to break up the stone, can be predicted explicitly. The main result is to determine the influence of the stress concentrations on the ultimate resistance to breakup of the stone. Hopefully this will begin a theoretical discussion of the relative ease of breaking different types of stones as a function of the microstructure. This has been a subject of experimental inquiry by a number of authors,[5,6] see also the review by Coleman and Saunders.[4]

Correspondence to: Andrew Szeri (e-mail: Andrew.Szeri@berkeley.edu)
Contract grant sponsor: U.S. National Science Foundation Program in Biomedical Engineering.

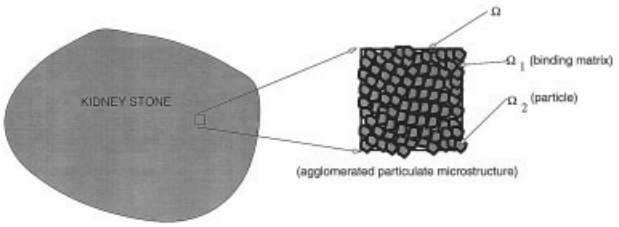

Figure 1. A schematic of a kidney stone formed by agglomerated particles.

MICROMECHANICAL CHARACTERIZATION OF A HETEROGENEOUS STONE

Structure and Morphology of Heterogeneous Stones

Kidney stones consist of an agglomeration of crystalline materials interspersed with an organic matrix of fibrous quality.[4,5,7] The crystalline phase is usually calcium oxalate monohydrate (COM) ($CaC_2O_4H_2O$), calcium oxalate dihydrate (COD), ($CaC_2O_42H_2O$), uric acid ($C_5H_4N_4O_3$), struvite ($MgNH_4PO_46H_2O$), or cystine ($—SCH_2CHNH_2COOH)_2$. The organic matrix appears to form from proteins that adsorb to the growing crystals.[8,9] It takes on the structure of a matted sheet between crystals in COM and COD stones.[10]

COM and uric acid stones have a concentric laminated structure in addition to to the crystal arrangement. They tend to break up by separation along the layers.[5] COM stones also tend to have well-defined radial striations associated with the crystal orientations within the stone.[9] COM stones are often highly disorganized in the stone center. COD stones show much less structure, unless there is significant COM present also.[10] Struvite is always present in stones in conjunction with calcium apatite; the stones are coarse grained but quite disorganized.[7] Struvite stones break differently from COM and uric-acid stones; they tend to fracture irregularly along crystal surfaces.[11] Cystine stones may have a finer-grained internal structure without laminations or radial striations, or they may be coarse grained. They are either very difficult or very easy to break up by SWL.[12]

Clearly there is a wide variation in the microstructure of heterogeneous kidney stones. Presently, there appears to be no adequate theory that ascertains the influence of microscale heterogeneity on the stress distributions under loading of kidney stones. The purpose of the present work is to develop a theoretical framework for formulating these problems. What is required is a tractable way of handling the solid mechanics that accounts for the presence of small-scale structure. For simplicity, this first effort considers stones that have a microstructure that can be characterized as random and isotropic, and linearly elastic in both phases. Therefore the present analysis might be expected to apply more directly to cystine and struvite stones, perhaps with some generosity to COD stones, and likely not particularly well to uric-acid and COM stones. The reason is that the latter compositions lead to large-scale structure and anisotropy that violates the simple assumptions that will be made in this first theory.

One difficulty is that in order to apply well-developed techniques, some unknown parameters are needed. A secondary purpose of the present work is to describe what kidney-stone measurements are needed in order to have a solid foundation for a sound theory. However, this will require improvisation in order to develop a concrete result. What has been measured is the sound speed through the crystalline material and the matrix of uric-acid stones; this was accomplished by acoustical measurements of *p*-wave speeds by Pittomvils et al.[13] —see also Reference 6. These data can be used to determine the bulk modulus of each phase. From the *p*-wave speed (c),

$$c = \sqrt{\frac{\lambda + 2\mu}{\rho}} \Rightarrow \lambda + 2\mu = c^2\rho, \tag{1}$$

where λ and μ are the Lamé parameters and ρ is the mass density. Thus, because $\lambda = \kappa - 2/3\mu$,

$$\kappa + \frac{4}{3}\mu = c^2\rho, \tag{2}$$

where κ is the bulk modulus. The shear moduli can be estimated by assuming that the material has a shear property similar to that of a ceramic, due to the polycrystalline nature of the materials involved. In other words, the ratio of bulk to shear moduli is a function of Poisson's ratio ν taken to be a representative value of $\nu = 0.35$. The relationship between κ and μ is

$$\frac{\kappa}{\mu} = \frac{2(1+\nu)}{3(1-2\nu)}; \tag{3}$$

thus $\kappa = 3\mu$. Consequently,

$$\kappa = \frac{1}{2}c^2\rho \quad \text{and} \quad \mu = \frac{1}{6}c^2\rho. \tag{4}$$

The values of c and ρ for each phase were given in Pittomvils et al.[13] With the parameters determined as indicated, the estimated moduli are shown in Table I. It is unfortunate that data for uric-acid stones must be used,[13] and yet the theory developed is more suitable for stones with an isotropic microstructure. However, that appears to be all that is available.

Notation

Before embarking on the theory, a word about notation is in order. Throughout this work, boldface symbols indicate vectors or tensors. The inner product of two vectors ($\mathbf{u}$) and ($\mathbf{v}$) is denoted $\mathbf{u} \cdot \mathbf{v}$. At the risk of oversimplification, the distinction between second-order tensors and matrices is ignored. Furthermore, a Cartesian basis exclusively employed. Readers may consult the texts of Malvern[14] and Marsden and Hughes[15] for background. Hence, if the second-order tensor $\mathbf{A}$ is considered, with its matrix representation

TABLE I. Material properties used in the present work, estimated from experimental data from ref. 13 as described in the text. The matrix has bulk and shear moduli of κ_1 and μ_1. The harder crystalline inclusions have bulk and shear moduli of κ_2 and μ_2. The volume fraction of the matrix v_2 is taken from ref. 13.

Material Property	Value
κ_1(GPa)	0.160
μ_1(GPa)	$\kappa_1/3$
κ_2(GPa)	14.973
μ_2(GPa)	$\kappa_2/3$
v_2	0.90

$$[\mathbf{A}] \overset{\text{def}}{=} \begin{bmatrix} A_{11} & A_{12} & A_{13} \\ A_{21} & A_{22} & A_{23} \\ A_{31} & A_{32} & A_{33} \end{bmatrix}, \tag{5}$$

then the product of two second-order tensors $\mathbf{A} \cdot \mathbf{B}$ is defined by the matrix product $[\mathbf{A}][\mathbf{B}]$, with components of $A_{ij}B_{jk} = C_{ik}$, where repeated indices imply summation. The scalar product of two tensors or matrices is $\mathbf{A} : \mathbf{B} = A_{ij}B_{ij} = \text{tr}\,([\mathbf{A}]^T[\mathbf{B}])$, where $\text{tr}\,(\cdot) = (\cdot)_{ii}$ is the trace operator. Finally, the divergence of a vector field $\mathbf{u}$ is defined by $\nabla \cdot \mathbf{u} = u_{i,i}$ —with a comma in the subscript denoting differentiation with respect to the ith coordinate; for a second-order tensor field $\mathbf{A}$, $\nabla \cdot \mathbf{A}$ describes a contraction to a vector with the components $A_{ij,j}$. With this preamble out of the way, a description of the effective material properties of the heterogeneous body is now given.

Micro–Macro Properties

A theory for the mechanics of microheterogeneous kidney stone will require knowledge of the overall effective mechanical properties of microheterogeneous materials, comprised of particles suspended in a binding matrix (Figure 1). Results from the well-developed theory of heterogeneous solids are used in order to determine overall properties. The theory is framed in terms of linear elastic fracture mechanics (LEFM). The basic assumption is that inelastic deformations occur in a region that is small compared to the size of developing cracks. When this is not so, as might be the case if there is significant plastic deformation over large areas of the binding matrix, one should use instead elastic plastic fracture mechanics (EPFM). If a rate-dependent theory is desired, one can make use of viscoelastic material models for the binding matrix or particulate phases. This comes at a significant increase in complexity with many more unknown parameters, and results in models that can only be numerically integrated.

$\mathbb{E}$ denotes the effective mechanical response (or stiffness) —a fourth-order elasticity tensor— described via the relation between average stress and strain fields: $\langle\sigma\rangle_\Omega = \mathbb{E}^* : \langle\varepsilon\rangle_\Omega$; in terms of components this is $\langle\sigma_{ij}\rangle_\Omega = E_{ijkl}^* \langle\varepsilon_{kl}\rangle_\Omega$. Here

$$\langle\cdot\rangle_\Omega \overset{\text{def}}{=} \frac{1}{|\Omega|}\int_\Omega \cdot\, d\Omega,$$

and σ and ε are the stress and strain tensor fields within a statistically representative volume element (RVE) of volume $|\Omega|$. The RVE will be discussed shortly. The domain of the matrix phase is Ω_1, and the domain of the particle phase is Ω_2. Of course, at the microscale, the mechanical properties of microheterogeneous materials are characterized by a spatially variable elasticity tensor $\mathbb{E}$. The effective response $\mathbb{E}^*$ is assumed isotropic, which obtains when the particles are randomly distributed and randomly oriented. An isotropic body has material properties that are the same in every direction at a point in the body; that is, the properties are not a function of orientation at a point in the body. It can be shown that when the body is isotropic, there are but two free constants in $\mathbb{E}^*$, which may be written compactly

$$\begin{Bmatrix} \langle\sigma_{11}\rangle_\Omega \\ \langle\sigma_{22}\rangle_\Omega \\ \langle\sigma_{33}\rangle_\Omega \\ \langle\sigma_{12}\rangle_\Omega \\ \langle\sigma_{23}\rangle_\Omega \\ \langle\sigma_{13}\rangle_\Omega \end{Bmatrix} = \underbrace{\begin{bmatrix} \kappa^* + \frac{4}{3}\mu^* & \kappa^* - \frac{2}{3}\mu^* & \kappa^* - \frac{2}{3}\mu^* & 0 & 0 & 0 \\ \kappa^* - \frac{2}{3}\mu^* & \kappa^* + \frac{4}{3}\mu & \kappa^* - \frac{2}{3}\mu^* & 0 & 0 & 0 \\ \kappa^* - \frac{2}{3}\mu^* & \kappa^* - \frac{2}{3}\mu^* & \kappa^* + \frac{4}{3}\mu^* & 0 & 0 & 0 \\ 0 & 0 & 0 & \mu^* & 0 & 0 \\ 0 & 0 & 0 & 0 & \mu^* & 0 \\ 0 & 0 & 0 & 0 & 0 & \mu^* \end{bmatrix}}_{\mathbb{E}^*} \begin{Bmatrix} \langle\varepsilon_{11}\rangle_\Omega \\ \langle\varepsilon_{22}\rangle_\Omega \\ \langle\varepsilon_{33}\rangle_\Omega \\ 2\langle\varepsilon_{12}\rangle_\Omega \\ 2\langle\varepsilon_{23}\rangle_\Omega \\ 2\langle\varepsilon_{13}\rangle_\Omega \end{Bmatrix}. \tag{6}$$

Here the effective bulk and shear moduli are given by

$$3\kappa^* \overset{\text{def}}{=} \left\langle \frac{tr\boldsymbol{\sigma}}{3} \right\rangle_\Omega \Big/ \left\langle \frac{tr\boldsymbol{\varepsilon}}{3} \right\rangle_\Omega \tag{7}$$

and

$$2\mu^* \overset{\text{def}}{=} \sqrt{\langle\boldsymbol{\sigma}'\rangle_\Omega : \langle\boldsymbol{\sigma}'\rangle_\Omega / \langle\boldsymbol{\varepsilon}'\rangle_\Omega : \langle\boldsymbol{\varepsilon}'\rangle_\Omega}, \tag{8}$$

where $\boldsymbol{\varepsilon}' = \boldsymbol{\varepsilon} - \frac{\text{tr}\boldsymbol{\varepsilon}}{3}\mathbf{1}$ is the deviatoric strain, σ' is the deviatoric stress, and $\mathbf{1}$ is the second-order identity tensor. In this case one may write

$$\mathbb{E}^*:\langle\boldsymbol{\varepsilon}\rangle_\Omega = 3\kappa^*\left\langle\frac{tr\,\boldsymbol{\varepsilon}}{3}\right\rangle_\Omega \mathbf{1} + 2\mu^*\langle\boldsymbol{\varepsilon}'\rangle_\Omega. \tag{9}$$

The eigenvalues of an isotropic effective elasticity tensor are $(3\kappa^*, 2\mu^*, 2\mu^*, \mu^*, \mu^*, \mu^*)$. Therefore, it is necessary to have $\kappa^* > 0$ and $\mu^* > 0$ to retain positive definiteness of $\mathbb{E}^*$, as is required by thermodynamic arguments. An extensive review of the analysis of random heterogeneous media can be found in the work of Torquato.[16–20]

It is clear that for concepts involving the relation between averages to be useful, they must be computed over a sample containing a statistically representative amount of material of volume $|\Omega|$. This size requirement can be made precise, as follows. A commonly accepted macro/micro criterion used in effective property calculations is Hill's condition;[21] $\langle\sigma : \varepsilon\rangle_\Omega : \langle\sigma\rangle_\Omega : \langle\varepsilon\rangle_\Omega$. This condition dictates the size requirements on the RVE. The classical argument is as follows. For any perfectly bonded heterogeneous body in the absence of body forces, two physically important loading states satisfy Hill's condition. They are (a) pure linear displacements of the form $\boldsymbol{u}|_{\partial\Omega} = \mathscr{E}\cdot\boldsymbol{x} \Rightarrow \langle\boldsymbol{\varepsilon}\rangle_\Omega = \mathscr{E}$, and (b) pure tractions in the form $\boldsymbol{t}|_{\partial\Omega} = \mathbf{L}\cdot\mathbf{n} \Rightarrow \langle\boldsymbol{\sigma}\rangle_\Omega = \mathbf{L}$; where $\mathscr{E}$ and $\mathbf{L}$ are constant strain and stress tensors, respectively. Clearly, for Hill's conditions to be satisfied within a macroscopic body under nonuniform external loading, the sample must be large enough to possess small boundary field fluctuations relative to its size. Therefore, applying (a)- or (b)-type boundary conditions to a large sample is a way of reproducing approximately what may be occurring in a statistically representative microscopic sample of material in a macroscopic body (Figure 1).

Struvite crystals tend to be up to roughly 20–50 μm in size; in cystine stones, the crystals are smaller —roughly up to 10 μm in size[7] in smooth cystine stones.[12] It has been estimated that, for the class of microstructures considered, the RVE should be such that in contains between 100 and 1000 particles. For example, see Lemaitre and Chaboche,[22] Huet,[23] Zohdi[24] or Zohdi and Wriggers.[25] Thus, roughly a (cubical) RVE should contain 5 to 10 particles on a side.

This may be compared to the length scale of a shock. If the rise time of a shock in water is taken to be 10 ns, then the thickness of the shock is about 15 μm in water, and perhaps 40 μm in the stone interior. Hence the size of the RVE may be approaching the length scale of the wave front, but is much, much smaller than either the compression or the rarefaction part of the wave. A higher-resolution theory would have to be fully numerical, as in References[24, 26, and 27]. It is worth emphasizing that in this work, damage is characterized in an overall sense. Local failure mechanisms are inaccessible.

Estimates of the Effective Bulk and Shear Moduli in Terms of Phase Properties

The constitutive tensor $\mathbb{E}^*$ provides the macroscale constitutive properties of a microheterogeneous material because it yields mapping between the average stress and strain measures. Until recently, the direct computation of micromaterial responses was very difficult. Accordingly, classical approaches have sought to approximate or bound effective responses. A widely used set of estimates for the effective properties are the Hashin-Shtrikman bounds[28,29] for isotropic materials with isotropic effective responses; for the bulk moduli

$$\kappa^{*,-} \overset{\text{def}}{=} \kappa_1 + \frac{\upsilon_2}{\left(\frac{1}{\kappa_2-\kappa_1} + \frac{3(1-\upsilon_2)}{3\kappa_1+4\mu_1}\right)} \le \kappa^* \le \kappa_2 + \frac{(1-\upsilon_2)}{\left(\frac{1}{\kappa_1-\kappa_2} + \frac{3\upsilon_2}{3\kappa_2+4\mu_2}\right)} \overset{\text{def}}{=} \kappa^{*,+}, \tag{10}$$

and for the shear moduli

$$\mu^{*,-} \overset{\text{def}}{=} \mu_1 + \frac{\upsilon_2}{\left(\frac{1}{\mu_2-\mu_1} + \frac{6(1-\upsilon_2)(\kappa_1+2\mu_1)}{5\mu_1(3\kappa_1+4\mu_1)}\right)} \le \mu^* \le \mu_2 + \frac{(1-\upsilon_2)}{\left(\frac{1}{\mu_1-\mu_2} + \frac{6\upsilon_2(\kappa_2+2\mu_2)}{5\mu_2(3\kappa_2+4\mu_2)}\right)} \overset{\text{def}}{=} \mu^{*,+}, \tag{11}$$

where $\kappa_2 \ge \kappa_1$ are the bulk moduli and $\mu_2 \ge \mu_1$ are the shear moduli of the particle and binder phases, respectively, and υ_2 is the volume fraction of particles; of course the volume fraction of the matrix is υ_1, where $\upsilon_1 + \upsilon_2 = 1$. Such bounds are the tightest known (perhaps tightest possible) on isotropic effective responses, with isotropic two-phase microstructures, where only the volume fractions and phase contrasts of the constituents are known. Note that no further geometric information, such as the number and nature of asperities, etc, contributes to these bounds.

A straightforward estimate of the effective properties is to take a convex combination of the bounds; for example,

$$\kappa^* \approx \theta\kappa^{*,+} + (1-\theta)\kappa^{*,-} \quad \text{and} \quad \mu^* \approx \theta\mu^{*,+} + (1-\theta)\mu^{*,-}, \tag{12}$$

where $0 \le \theta \le 1$. In the present work, because hard particulates are surrounded by a soft matrix, the properties of the matrix control the effective properties, despite the fact that it is of much smaller volume fraction. Here $\theta = 0.25$. Detailed experimental and analytical work on how to estimate θ can be found in Zohdi et al.[30] In short, for microstructures comprised of hard particles surrounded by a continuous soft matrix, which produces an overall stiffness that is significantly smaller than the reverse, a hard matrix encasing soft particles, it is well known that the Hashin-Shtrikman lower bound is quite accurate;[31] this motivates the choice of $\theta = 0.25$. Note that θ is a property of the material —measurable or calculable— and not a free parameter. Because it is associated with

the material, all of the material properties are computed with the same θ.

Load Sharing Between the Two Phases

The load carried by each phase in the microstructure is characterized via stress concentration tensors, which are now discussed. These provide a measure of the deviation away from the mean fields throughout the material. One can decompose averages of an arbitrary quantity over Ω into averages over the each of the phases in the following manner:

$$\langle \mathbf{A} \rangle_{\Omega} = \frac{1}{|\Omega|} \left(\int_{\Omega_1} \mathbf{A}\, d\Omega + \int_{\Omega_2} \mathbf{A}\, d\Omega \right) = v_1 \langle \mathbf{A} \rangle_{\Omega_1} + v_2 \langle \mathbf{A} \rangle_{\Omega_2}. \tag{13}$$

This decomposition leads to

$$\langle \boldsymbol{\sigma} \rangle_{\Omega} = v_1 \langle \boldsymbol{\sigma} \rangle_{\Omega_1} + v_2 \langle \boldsymbol{\sigma} \rangle_{\Omega_2} = v_1 \mathbb{E}_1 : \langle \boldsymbol{\varepsilon} \rangle_{\Omega_1} + v_2 \mathbb{E}_2 : \langle \boldsymbol{\varepsilon} \rangle_{\Omega_2}.$$

Substitution of the identity $\langle \boldsymbol{\varepsilon} \rangle_{\Omega 1} = \langle \boldsymbol{\varepsilon} \rangle_{\Omega} - v_2 \langle \boldsymbol{\varepsilon} \rangle_{\Omega 2}$ leads to

$$v_1 \mathbb{E}_1 : \langle \boldsymbol{\varepsilon} \rangle_{\Omega_1} + v_2 \mathbb{E}_2 : \langle \boldsymbol{\varepsilon} \rangle_{\Omega_2} = \mathbb{E}_1 : (\langle \boldsymbol{\varepsilon} \rangle_{\Omega} - v_2 \langle \boldsymbol{\varepsilon} \rangle_{\Omega_2}) + v_2 \mathbb{E}_2 : \langle \boldsymbol{\varepsilon} \rangle_{\Omega_2}.$$

The entire expression may then be rewritten as one involving a premultiplier of $\langle \boldsymbol{\varepsilon} \rangle_{\Omega}$:

$$\langle \boldsymbol{\sigma} \rangle_{\Omega} = \mathbb{E}_1 : (\langle \boldsymbol{\varepsilon} \rangle_{\Omega} - v_2 \langle \boldsymbol{\varepsilon} \rangle_{\Omega_2}) + v_2 \mathbb{E}_2 : \langle \boldsymbol{\varepsilon} \rangle_{\Omega_2} = ((\mathbb{E}_1 + v_2 (\mathbb{E}_2 - \mathbb{E}_1)) : \mathbf{C}) : \langle \boldsymbol{\varepsilon} \rangle_{\Omega_1}$$

where $\mathbf{C}$**:** $\langle \boldsymbol{\varepsilon} \rangle_{\Omega} = \langle \boldsymbol{\varepsilon} \rangle_{\Omega_2}$, *with*

$$\mathbf{C} \overset{\text{def}}{=} \left(\frac{1}{v_2} (\mathbb{E}_2 - \mathbb{E}_1)^{-1} : (\mathbb{E}^* - \mathbb{E}_1) \right).$$

The strain concentration tensor $\mathbf{C}$ relates the average strain over the particle phase (2) to the average strain over all phases. Similarly, for the variation in the stress, $\mathbf{C}$ **:** $\mathbb{E}^{*-1} : \langle \boldsymbol{\sigma} \rangle_{\Omega} = \mathbb{E}_2{}^{-1} : \langle \boldsymbol{\sigma} \rangle_{\Omega_2}$, which reduces to

$$\mathbb{E}_2 : \mathbf{C} : \mathbb{E}^{*-1} : \langle \boldsymbol{\sigma} \rangle_{\Omega} \overset{\text{def}}{=} \bar{\mathbf{C}} : \langle \boldsymbol{\sigma} \rangle_{\Omega} = \langle \boldsymbol{\sigma} \rangle_{\Omega_2}. \tag{14}$$

$\bar{\mathbf{C}}$ is known as the stress concentration tensor; it relates the average stress in the particle phase to that in the whole RVE. Note that once either $\bar{\mathbf{C}}$ or $\mathbb{E}^*$ are known, the other can be determined.

In the case of isotropy

$$\bar{C}_{\kappa} \overset{\text{def}}{=} \frac{1}{v_2} \frac{\kappa_2}{\kappa^*} \frac{\kappa^* - \kappa_1}{\kappa_2 - \kappa_1} \quad \text{and} \quad \bar{C}_{\mu} \overset{\text{def}}{=} \frac{1}{v_2} \frac{\mu_2}{\mu^*} \frac{\mu^* - \mu_1}{\mu_2 - \mu_1}, \tag{15}$$

where

$$\bar{C}_k \left\langle \frac{tr \boldsymbol{\sigma}}{3} \right\rangle_{\Omega} = \left\langle \frac{tr \boldsymbol{\sigma}}{3} \right\rangle_{\Omega_2}$$

and where $\bar{C}_{\mu} \langle \boldsymbol{\sigma}' \rangle_{\Omega} = \langle \boldsymbol{\sigma}' \rangle_{\Omega_2}$. Clearly, the microstress fields are minimally distorted when $\bar{C}_k = \bar{C}_{\mu} = 1$; there are no stress concentrations in a homogeneous material, for homogeneous loading. For the matrix,

$$\langle \boldsymbol{\sigma} \rangle_{\Omega_1} = \frac{\langle \boldsymbol{\sigma} \rangle_{\Omega} - v_2 \langle \boldsymbol{\sigma} \rangle_{\Omega_2}}{v_1} = \frac{\langle \boldsymbol{\sigma} \rangle_{\Omega} - v_2 \bar{C} : \langle \boldsymbol{\sigma} \rangle_{\Omega}}{v_1} = \frac{(1 - v_2 \bar{C}) : \langle \boldsymbol{\sigma} \rangle_{\Omega}}{v_1} \overset{\text{def}}{=} C : \langle \boldsymbol{\sigma} \rangle_{\Omega}. \tag{16}$$

Therefore, in the case of isotropy,

$$\overset{=}{C}_{\kappa} \overset{\text{def}}{=} \frac{1}{v_1} (1 - v_2 \bar{C}_{\kappa}) \quad \text{and} \quad \overset{=}{C}_{\mu} \overset{\text{def}}{=} \frac{1}{v_1} (1 - v_2 \bar{C}_{\mu}). \tag{17}$$

The utility of such relations is that they allow one to determine what the load sharing is for each phase. Typically, for kidney stones, the failure of the matrix that binds the particulates together is of interest. However, the theory developed here can be applied to estimate failure of the matrix or of the particulates.

FATIGUE-LIFE ESTIMATES FOR THE DESTRUCTION OF KIDNEY STONES

The classical Basquin relation is employed for fatigue-life estimation, which is as follows at a material point.[32]

$$\| \boldsymbol{\sigma}_a \| = (\| \boldsymbol{\sigma}_f \| - \| \boldsymbol{\sigma}_m \|)(2N_f)^b \Rightarrow N_f = \frac{1}{2} \left(\frac{\| \boldsymbol{\sigma}_a \|}{\| \boldsymbol{\sigma}_f \| - \| \boldsymbol{\sigma}_m \|} \right)^{1/b}, \tag{18}$$

where $\| \boldsymbol{\sigma} \| \overset{\text{def}}{=} \sqrt{\boldsymbol{\sigma} : \boldsymbol{\sigma}}$. Here the norm of the mean stress is $\| \boldsymbol{\sigma}_m \| = \| \boldsymbol{\sigma}_{max} + \boldsymbol{\sigma}_{min} \| / 2$, and the norm of the fluctuating stress is $\| \boldsymbol{\sigma}_a \| = \| \boldsymbol{\sigma}_{max} - \boldsymbol{\sigma}_{min} \| / 2$. Static failure stress is denoted by $\boldsymbol{\sigma}_f$ and, typically for most known materials, $-0.12 \leq b \leq -0.05$. Classical relations of this type are discussed in Suresh.[33] Classical approaches are followed here, and $\boldsymbol{\sigma}_f$ is set to be the minimum of the absolute values of the failure stresses in tension or compression, when these differ.

This is extended to overall failure of each of the phases by using volumetric averages over each phase. For the second

(particle) phase, the overall number of cycles to failure for the particle phase (2) is*

$$N_{f2} = \frac{1}{2}\left(\frac{\|\langle\boldsymbol{\sigma}_a\rangle_{\Omega_2}\|}{\|\langle\boldsymbol{\sigma}_f\rangle_{\Omega_2}\| - \|\langle\boldsymbol{\sigma}_m\rangle_{\Omega_2}\|}\right)^{1/b_2} = \frac{1}{2}\left(\frac{\|\bar{\mathbf{C}}:\langle\boldsymbol{\sigma}_a\rangle_{\Omega}\|}{\|\langle\boldsymbol{\sigma}_f\rangle_{\Omega_2}\| - \|\bar{\mathbf{C}}:\langle\boldsymbol{\sigma}_m\rangle_{\Omega}\|}\right)^{1/b_2}, \tag{19}$$

whereas for the binding matrix phase (1)

$$N_{f1} = \frac{1}{2}\left(\frac{\|\langle\boldsymbol{\sigma}_a\rangle_{\Omega_1}\|}{\|\langle\boldsymbol{\sigma}_f\rangle_{\Omega_1}\| - \|\langle\boldsymbol{\sigma}_m\rangle_{\Omega_1}\|}\right)^{1/b_1} = \frac{1}{2}\left(\frac{\|\bar{\mathbf{C}}:\langle\boldsymbol{\sigma}_a\rangle_{\Omega}\|}{\|\langle\boldsymbol{\sigma}_f\rangle_{\Omega_1}\| - \|\bar{\bar{C}}:\langle\boldsymbol{\sigma}_m\rangle_{\Omega}\|}\right)^{1/b_1}. \tag{20}$$

The rates of increase and decrease of the fatigue lives are controlled by the magnitudes of the b_i's.

Consistent with the use of effective (volumetrically averaged) properties, a body is considered with an idealized loading on its boundary of the form $\mathbf{t}|_{\partial\Omega} = \mathbf{L}\cdot\mathbf{n}$, where $\mathbf{t}$ is the surface traction, $\mathbf{L}$ is a second-order (load) tensor, and $\mathbf{n}$ is the outward unit normal on the boundary $\partial\Omega$. Consistent with classical fatigue theory, inertial effects are neglected. The identity $\nabla\cdot(\boldsymbol{\sigma}\otimes\mathbf{x}) = (\nabla\cdot\boldsymbol{\sigma})\otimes\mathbf{x} + \boldsymbol{\sigma}\cdot\nabla\mathbf{x} = \boldsymbol{\sigma}$ is used where $\mathbf{x}$ is the position vector of an arbitrary point within the body, and $\otimes$ is the dyadic product. This is substituted into the definition of the average stress to obtain (using Gauss's divergence theorem)

$$\langle\boldsymbol{\sigma}\rangle_{\Omega} = \frac{1}{|\Omega|}\int_{\Omega}\nabla\cdot(\boldsymbol{\sigma}\otimes\mathbf{x})\,d\Omega = \frac{1}{|\Omega|}\int_{\partial\Omega}(\boldsymbol{\sigma}\otimes\mathbf{x})\cdot\mathbf{n}\,da$$

$$= \frac{1}{|\Omega|}\int_{\partial\Omega}(\mathbf{L}\otimes\mathbf{x})\cdot\mathbf{n}\,da = \mathbf{L}$$

For simplicity, pressure-like loading on the surface of the RVE in the form

$$\boldsymbol{t}|_{\partial\Omega} \overset{\text{def}}{=} \underbrace{\begin{bmatrix} L & 0 & 0 \\ 0 & L & 0 \\ 0 & 0 & L \end{bmatrix}}_{\langle\boldsymbol{\sigma}\rangle_{\Omega} = L}\begin{bmatrix} n_1 \\ n_2 \\ n_3 \end{bmatrix}. \tag{21}$$

is considered. With this loading, all states which satisfy the failure criterion for the matrix satisfy

$$N_{f1} = \frac{1}{2}\left(\frac{\|\langle\boldsymbol{\sigma}_a\rangle_{\Omega_1}\|}{\|\langle\boldsymbol{\sigma}_f\rangle_{\Omega_1}\| - \|\langle\boldsymbol{\sigma}_m\rangle_{\Omega_1}\|}\right)^{1/b_1} = \frac{1}{2}\left(\frac{\|\bar{\bar{C}}:\langle\boldsymbol{\sigma}_a\rangle_{\Omega}\|}{\|\langle\boldsymbol{\sigma}_f\rangle_{\Omega_1}\| - \|\bar{\bar{C}}:\langle\boldsymbol{\sigma}_m\rangle_{\Omega}\|}\right)^{1/b_1}. \tag{22}$$

Of course, the RVE experiences both dilatational and deviatoric loading. Stress concentrations for both dilatational and deviatoric loading have been developed. With a suitable mesoscopic model that includes full coupling between the fluid and stone one could be definite about what loading to prescribe on the RVE. Such a model does not yet exist. This first examination of the influences of stress concentrations associated with microscale heterogeneity will focus on mesoscopic loading of the following form: $\langle\boldsymbol{\sigma}_{max}\rangle_{\Omega} = A\langle\boldsymbol{\sigma}_f\rangle_{\Omega_1}$ (tension, $A > 0$) and $\langle\boldsymbol{\sigma}_{min}\rangle_{\Omega} = B\langle\boldsymbol{\sigma}_f\rangle_{\Omega_1}$ (compression, $B < 0$), with a normalization of

$$\langle\boldsymbol{\sigma}_f\rangle_{\Omega_1} = \sigma_f\begin{bmatrix} 1 & 0 & 0 \\ 0 & 1 & 0 \\ 0 & 0 & 1 \end{bmatrix}. \tag{23}$$

Here σ_f is the failure stress of the binding matrix. Note that here the focus is on Mode I (opening mode) of microcrack growth due to fatigue, hence the form of the loading considered. Therefore, the amplitude of the alternating stress is

$$\langle\boldsymbol{\sigma}_a\rangle_{\Omega} = \frac{A-B}{2}\langle\boldsymbol{\sigma}_f\rangle_{\Omega_1}, \tag{24}$$

and the mean is

$$\langle\boldsymbol{\sigma}_m\rangle_{\Omega} = \frac{A+B}{2}\langle\boldsymbol{\sigma}_f\rangle_{\Omega_1} \tag{25}$$

Thus, if the previous expressions are substituted into (22), the relationship between N_{f1}, A, and B becomes

$$N_{f1} = \frac{1}{2}\left(\frac{\bar{\bar{C}}_{\kappa}\frac{|A-B|}{2}}{1 - \bar{\bar{C}}_{\kappa}\frac{|A+B|}{2}}\right)^{1/b_1}, \tag{26}$$

where, due to the *overall hydrostatic loading,* the overall failure depends on only the bulk modulus concentration factor, and on the maximum and minimum averaged dimensionless stresses. Note that in an overall, volumetrically averaged sense, overall deviatoric stresses vanish, and local deviatoric failures cannot be resolved, due to the type of loading considered, that is, Mode I opening of a microscale crack.

The number of cycles to failure versus maximum (dimensionless) tension $A > 0$ and compression $B < 0$ per cycle is plotted in Figure 2, using material properties found in Table I. The fatigue exponent b_1 was chosen to be the average of the ranges cited earlier $-0.085 = -(0.12 + 0.05)/2$. It is emphasized that b_1 is a material property —measurable or calculable—and not a free parameter, in principle. These results for the number of cycles to failure fall within the ranges typically needed for the destruction of kidney stones ($10^2 - 10^3$). With the parameters determined as indicated, it was

*The compact notation is employed: $\langle\boldsymbol{\sigma}\rangle_{\Omega_1} = \left\langle\frac{tr\,\boldsymbol{\sigma}}{3}\right\rangle_{\Omega_1}\mathbf{1} + \langle\boldsymbol{\sigma}'\rangle_{\Omega_1} = \bar{C}_{\kappa}\left\langle\frac{tr\,\boldsymbol{\sigma}}{3}\right\rangle_{\Omega}\mathbf{1} + \bar{\bar{C}}_{\mu}\langle\boldsymbol{\sigma}'\rangle_{\Omega} \overset{\text{def}}{=} \bar{\bar{C}}:\langle\boldsymbol{\sigma}\rangle_{\Omega}$.

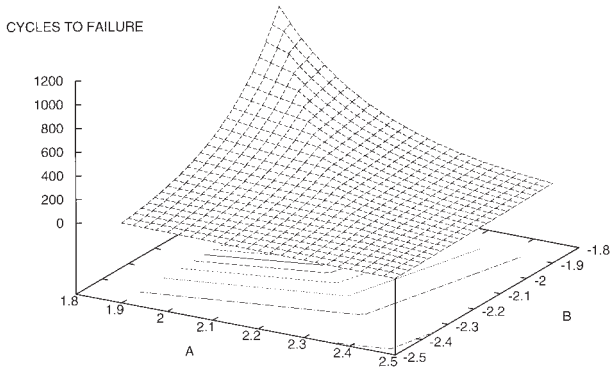

Figure 2. The relationship between the dimensionless maximum tension A and compression B and the number of cycles to binding matrix failure (N_{f1}) for $\theta = 0.25$. Contours of equal N_{f1} are shown on the plane.

found that $\overline{\overline{C}}_{\kappa} = 0.273$. The value of $\overline{\overline{C}}_{\mu}$ is irrelevant due to the overall purely hydrostatic stress state. This implies that the external loading, characterized by A and B will induce significantly smaller loads on the softer binding matrix than on the harder inclusions. Therefore, the peak stresses made dimensionless by the matrix failure stress. A and B, must be significantly greater than unity to induce failure of the matrix.

If the reasoning of Cohen and Whitfield[34] is followed, then the magnitudes may be reckoned in this way. From Figure 2, one can see that about 350 cycles are required to fragment a stone if $A = -B \approx 2.3$. If the matrix failure stress in tension is 5 bar, then $A = -B \approx 2.3$ corresponds to maximum and minimum stresses of roughly 10 bar. Owing to energy losses at the stone–fluid interface, this is associated with a liquid pressure of at least three times, or 30 bar. Finally, attenuation of the shock wave as it travels through (say 10 cm of) tissue would require a pulse of about 10 times that amount, or 30 MPa. This is within the range of lithotripters, although likely it is true that $A \neq -B$.

Of course, the nature of the cyclic loading at any one point in the stone is best derived from a mesoscopic model that accounts for coupling to the surrounding medium, and reflection and interaction of stress waves. Such a model for pressure waves in a homogeneous material was recently developed by Cleveland and Tello.[35] As one would expect, if the mean stress is increased, the alternating stress can be decreased to induce fatigue failure. Furthermore, if it is possible to increase the number of cycles, one can decrease the intensity of the mean and alternating stresses.

Some statements can be made about the influence of b_1 and θ on the fatigue surface shown in Figure 2. Alteration of b_1 changes the slope of the surface; whereas changes in θ shift it up or down dramatically; see Figure 3. Hence these two parameters, once measured, are essential ingredients in a sound theory.

DISCUSSION AND CONCLUSIONS

In the course of this work a number of approximations and estimates were made. The goal was to develop a theoretical framework capable of handling the mechanics of microheterogeneous kidney stones. To that end, an isotropic, random microstructure with two phases—particulate and binder—was considered. Stress concentration functions were developed to determine load sharing between the particle phase and the binding matrix phase. To illustrate application of the theory, fatigue-life estimates were developed for each phase, as a function of the volume fraction and of the mechanical properties of the constituents, as well as the mean and fluctuating loading. The failure of the binding matrix could then be predicted explicitly.

Measurements of laminated uric-acid stones[13] were used to estimate properties of matrix and binder, although this analysis applies more directly to struvite and cystine stones. Needless to say, the theory could be improved significantly by property measurements in a variety of stones. The analysis has also made use of a number of approximations. There remain material properties that could be measured in an experiment. These include the fatigue parameters in each phase b_i and the weighting θ in the mean property estimates. Some methods for determination of these parameters from experiments have been described.[30] Of course, it would also be useful to measure directly the bulk and shear moduli of the binding matrix and particulate phases; then one would not have to resort to determination of these quantities by the methods used earlier. Finally, it would be worthwhile to measure the failure stress for both matrix and particulate phases, in order to yield quantitative estimates for fatigue

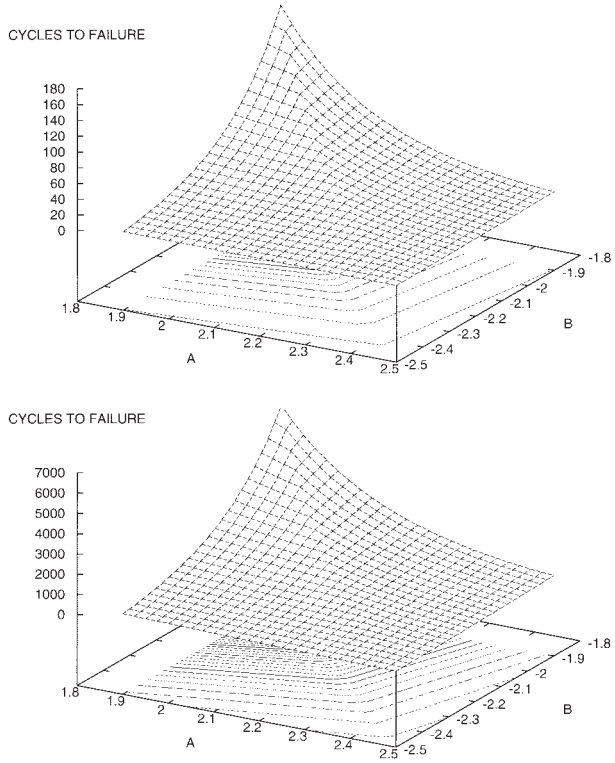

Figure 3. Number of cycles to binding matrix failure (N_{f1}) versus maximum tension A and compression B for $\theta = 0.2$ (upper) and 0.3 (lower).

failure. The approach presented here can serve as a precursor to more elaborate large-scale computational simulations, such as those found in Zohdi.[24, 26, 27] The assumption of isotropy could be relaxed, as estimates for certain anisotropic responses can be found in Hashin.[31] This would allow one to treat a greater variety of stones.

With a deeper understanding of the differences in the destruction of kidney stones of different types, one could possibly tailor the number and intensity of cycles of loading based on the type of stones. *In vivo,* one could imagine that the morphology could be determined by inverse methods, such as x-ray tomography. Such information could be used to obtain more precise estimates of the material properties, for use in a model that would estimate the number of cycles to failure. One can target chemical alteration of the stone with a goal toward further weakening it to enhance the action of shock-wave lithotripsy,[36] in a way that could be understood with a theory of the kind presented here. If, for example, the particulate phase is weakened, particulates will carry a smaller fraction of the load, hence weakening the stone.

The authors to thank P. Zhong for a stimulating discussion.

REFERENCES

1. Coleman AJ, Saunders JE, Crum LA, Dyson M. Acoustic cavitation generated by an extracorporeal shockwave lithotripter. Ultrasound Med Biol 1987;13:69–76.
2. Zhu SL, Cocks FH, Preminger GM, Zhong P. The role of stress waves and cavitation in stone comminution in shock wave lithotripsy. Ultrasound Med Biol 2002;28:661–671.
3. Lokhandwalla M, Sturtevant B. Fracture mechanics model of stone comminution in ESWL and implications for tissue damage. Phys Med Biol 2000;45:1923–1940.
4. Coleman AJ, Saunders JE. A review of the physical properties and biological effects of the high amplitude acoustic fields used in extracorporeal lithotripsy. Ultrasonics 1993;31:75–89.
5. Pittomvils G, Vanduersen H, Wevers M, Lafaut JP, De Ridder D, De Meester P, Boving R, Baert L. The influence of internal stone structure on the fracture behavior of urinary calculi. Ultrasound Med Biol 1994;20:803–810.
6. Sylven ET, Agarwal S, Briant CL, Cleveland RO. High strain rate testing of kidney stones. J Mater Sci Mater Med 2004;15: 613–617.
7. Kim KM. The stones. Scanning Electron Microsc. 1982;1635–1660.
8. Khan SR, Finlayson B, Hackett RL. Stone matrix as proteins adsorbed on crystal surfaces: a microscopic study. Scanning Electron Microsc 1983;1983:379–385.
9. Khan SR, Hackett RL. Role of organic matrix in urinary stone formation: an ultrastructural study of crystal matrix interface of calcium oxalate monohydrate stones. J Urol 1993;150:239–245.
10. Khan SR, Hackett RL. Microstructure of decalcified human calcium oxalate urinary stones, Scanning Electron Microsc 1984;935–941.
11. Khan SR, Hackett RL, Finlayson B. Morphology of urinary stone particles resulting from ESWL treatment. J Urol 1986; 136:1367–1372.
12. Bhatta KM, Prien Jr. EL, Dretler SP. Cystine calculi— rough and smooth: a new clinical distinction. J. Urol 1989;142:937–940.
13. Pittomvils G, Lafaut JP, Vandeursen H, Boving R, Baert L, Wevers M. Ultrasonic parameters of concentric laminated uric acid stones. Ultrasonics 1995;33:463–467.
14. Malvern L. Introduction to the mechanics of a continuous medium. Englewood Cliffs, NJ: Prentice Hall; 1968.
15. Marsden JE, Hughes TJR. Mathematical foundations of elasticity. Englewood Cliffs, NJ: Prentice Hall; 1983.
16. Torquato S. Random heterogeneous media: microstructure and improved bounds on effective properties. Appl Mech Rev 1991; 44:37–76.
17. Torquato S. Effective stiffness tensor of composite media I. Exact series expansions. J Mech Phys Sol 1997;45:1421–1448.
18. Torquato S. Effective stiffness tensor of composite media II. Applications to isotropic dispersions. J Mech Phys Sol 1998; 46:1411–1440.
19. Torquato S. Random heterogeneous materials: Microstructure and macroscopic properties. New York: Springer; 2002.
20. Torquato S, Hyun S. Effective-medium approximation for composite media: Realizable single-scale dispersions. J Appl Phys 2001;89:1725–1729.
21. Hill R. The elastic behaviour of a crystalline aggregate. Proc Phys Soc London Ser A 1952;65:349–359.
22. Lemaitre J, Chaboche JL. Mechanics of solid materials. Cambridge: Cambridge University Press; 1990.
23. Huet C. An integrated micromechanics and statistical continuum thermodynamics approach for studying the fracture behaviour of microcracked heterogeneous materials with delayed response. Eng Frac Mech Spec Iss 1997;58:459–556.
24. Zohdi TI. Genetic optimization of statistically uncertain microheterogeneous solids. Philos Trans R Soc Math Phys Sci Eng 2003;361:1021–1043.
25. Zohdi TI, Wriggers P. Computational micro–macro material testing. Arch Comp Meth Eng 2001;8:131– 228.
26. Zohdi TI. Constrained inverse formulations in random material design. Comp Meth Appl Mech Eng 2003;192:28–30, 18, 3179–3194.
27. Zohdi TI. Modeling and simulation of a class of coupled thermo-chemo-mechanical processes in multiphase solids. Comp Meth Appl Mech Eng 2004;193:679–699.
28. Hashin Z, Shtrikman S. (1962) On some variational principles in anisotropic and nonhomogeneous elasticity. J Mech Phys Solids 1962;10:335–342.
29. Hashin, Z., & Shtrikman, S. A variational approach to the theory of the elastic behaviour of multiphase materials. J Mech Phys Sol 1963;11:127–140.
30. Zohdi TI, Monteiro PJM, Lamour V. Extraction of elastic moduli from granular compacts. Int J Frac/Lett Micromech 2002;115:L49–L54.
31. Hashin Z. Analysis of composite materials: a survey. ASME J Appl Mech 1983;50:481–505.
32. Basquin OH. The exponential law of endurance tests. Proc Am Soc Test Mater 1910;10:625–630.
33. Suresh S. Fatigue of materials (2nd ed.). Cambridge: Cambridge University Press; 1998.
34. Cohen NP, Whitfield HN. Mechanical testing of urinary calculi. World J Urol 1993;11:13–18.
35. Cleveland RO, Tello JS. Effect of the diameter and the sound speed of a kidney stone on the acoustic field induced by shock waves. Acoust Res Lett Online 2004;5:37–43.
36. Heimbach D, Kourambas J, Zhong P, Jacobs J, Hesse A, Mueller SC, Delvecchio FC, Cocks FH, Preminger GM. The use of chemical treatments for improved comminution of artificial stones. J Urol 2004;171:1797–1801.